View metadata, citation and similar papers at core.ac.uk

brought to you by CORE

provided by Elsevier - Publisher Connector

A Model for Enhanced Nucleation of Protein Crystals on a Fractal Porous Substrate

S. Stolyarova,* E. Saridakis,†‡ N. E. Chayen,† and Y. Nemirovsky*

*Solid State Institute, Technion-Israel Institute of Technology, Haifa 32000, Israel; †Biological Structure and Function Section, Division of Biomedical Sciences, Faculty of Medicine, Imperial College, London SW7 2AZ, United Kingdom; and ‡Laboratory of Structural and Supramolecular Chemistry, Institute of Physical Chemistry, National Centre for Scientific Research 'Demokritos', Aghia Paraskevi, 15310 Athens, Greece

ABSTRACT The phenomenon of enhanced nucleation and crystallization of proteins on porous silicon (PS) is theoretically studied and explained. The PS layer is treated as a fractal structure, and a new mechanism of local supersaturation associated with the fractality is proposed. It is shown that the number of adsorbed molecules on a fragment with a fractal surface significantly exceeds that on one with flat surfaces. For a fractal PS surface, a local concentration of molecules that is sufficient for nucleation is possible inside and in the close vicinity of the pores, even when the average conditions in the bulk of the solution correspond to metastability. The wide distribution of fractal pore size is favorable for the crystallization of a wide range of macromolecules using the same sample. In addition, the PS technology is very flexible, allowing tailoring the pore size and concentration as well as the fractal properties to specific proteins by changing the fabrication conditions.

INTRODUCTION

Protein crystallization is the main bottleneck in the determination of the three-dimensional (3D) structure of proteins (1). Hence, there is an urgent requirement for new methodology to aid protein crystal growth. A unique experimental approach involving the use of porous silicon (PS) as a crystallization promoter for protein molecules has been introduced (2). Several types of proteins have been crystallized on PS substrates at metastable conditions, regardless of their charge and size (2). An example of protein crystallized on the PS is shown in Fig. 1.

PS is a nanostructured material obtained from standard polished silicon wafer by electrochemical etching. PS consists of nanoscale-sized crystalline silicon wires and dots surrounded by voids. The structure of the PS layer can be seen in Fig. 2, which shows a scanning electron microscope (SEM) image of a PS cross section. Fig. 3 shows SEM and atomic force microscope (AFM) images of the PS external surface. It is found that apart from biological molecules, PS stimulates precipitation and crystallization of inorganic materials such as mineral species (3), silicon dioxide (4), and sol-gel derived ceramic films (5).

It is known that PS is a fractal object. This follows from the results of various experiments and computer modeling (see, for example, (6–12)). The fractality means that the object is formed by parts that are 'similar' in some sense to the whole (13).The most important property of fractals is scale invariance, or scaling. Scaling means that any properties of the object are scaled in accordance with a definite rule: if one rescales the spatial dimension of the system L by a factor k, the property w (volume, resistance, mass, and so on) are rescaled by a factor k^{α}, i.e., $w(kL) = k^{\alpha}w(L)$ and α is not an integer, $\alpha \neq 1,2,3\ldots$. The solution of this functional equation is $w(L) = AL^{\alpha}$ where A is a constant and its dimensionality is $[A] = [w]/(\text{length})^{\alpha}$. Scaling exponents α are different for different properties. If the values of α are independent of the dilation direction i ($i = x$, y, or z), we have an isotropic, or self-similar, fractal. If the values of α depend on the dilation direction, the object possesses an anisotropic dilation symmetry; it is a self-affine fractal (13). In any case, a real-life fractal (as opposed to the mathematical object) has upper and lower cutoff lengths. The lower cutoff l represents the size of an elementary unit of the fractal structure. The upper cutoff L_c represents the size of a scaling region. For self-affine fractals, the value of L_c depends on the dilation direction i, $L_c = L_{ci}$. The upper cutoff of self-similarity L_c, called correlation length, appears to be due to the existence of finite correlation scales for any real fractal object. It is possible to say that any fractal structure is constituted from blocks with linear size L_{ci} and the number of these blocks is L_i/L_{ci} along each direction (here L_i is the linear size of the structure in the i-direction).

The fractal properties differ for various regions of PS since it has an intermediate structure between bulk self-similar fractals like silica gels and samples with rough self-affine fractal surface and monolithic bulk, such as appear as a result of deposition or erosion processes (14). The pore interior surface is formed by external surfaces of nanocrystallites constituting the porous layer. This surface is a self-similar fractal (6–8,12), i.e., it is scale-invariant along any direction up to the correlation length $L_{c,pore}$. This scale is of the order of the pore diameter (6–8) or the size of nanocrystallites constituting the porous layer (12). This statement can be related to

Submitted February 2, 2006, and accepted for publication July 6, 2006.

Address reprint requests to S. Stolyarova, Solid State Institute, Technion-Israel Institute of Technology, Haifa 32000, Israel. Tel.: 972-4-8293797; Fax: 972-4-8235107; E-mail: ssstolya@tx.technion.ac.il.

© 2006 by the Biophysical Society

0006-3495/06/11/3857/07 $2.00

doi: 10.1529/biophysj.106.082545

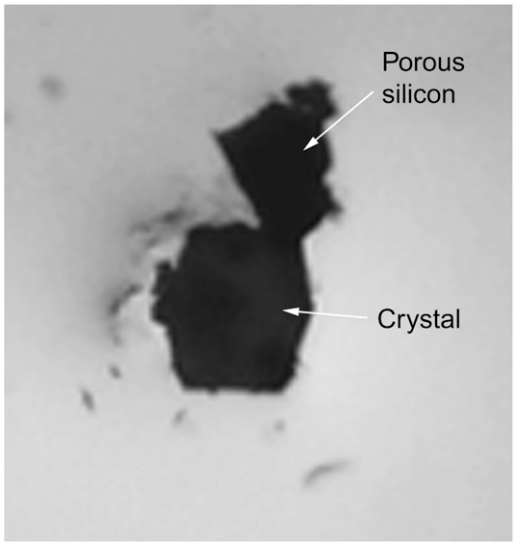

FIGURE 1 Single crysta1 of c-phycocyanin attached onto a PS fragment. Area shown is 0.5 × 0.5 mm. The crystallization method and conditions are described elsewhere (2).

any individual pore, i.e., there are many different values of $L_{c,pore}$ in accordance with the pore size distribution function.

In contrast with the pore interior surface, the external surface of the PS sample is a self-affine fractal (9,10), i.e., it has different scale-invariant properties along different directions (14). The external surface of the PS sample has one preferred direction perpendicular to the wafer surface. So, the self-affine fractal surface has two upper correlation lengths: the longitudinal L_{cl} in the (x,y) plane and the perpendicular L_{cp} in the z direction. L_{cp} characterizes the scale of the surface roughness. The surface can be described by the function $h(x,y)$, which gives its height at position (x,y) from a referent flat surface. The surface width $w(L)$ of a section of the surface having a size $L \times L$ in the referent plane is defined by the root mean square of the height fluctuation by $w(L) = (\langle h^2\rangle - \langle h\rangle^2)^{1/2}$. The averaging $\langle \ldots \rangle$ means integration over this section: $\langle h\rangle = L^{-2}\int h(x,y)dxdy$.

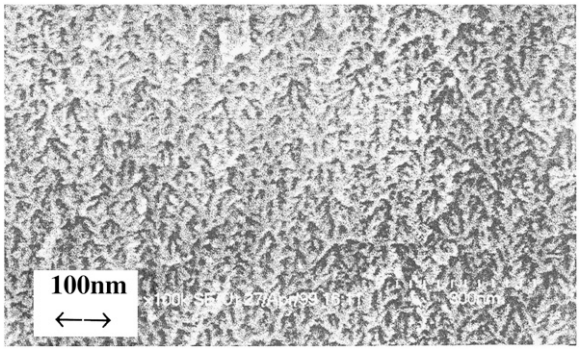

FIGURE 2 A cross section of p-type PS showing the structure of the material (tree-like); the silicon is white and the dark areas are pores in the layer.

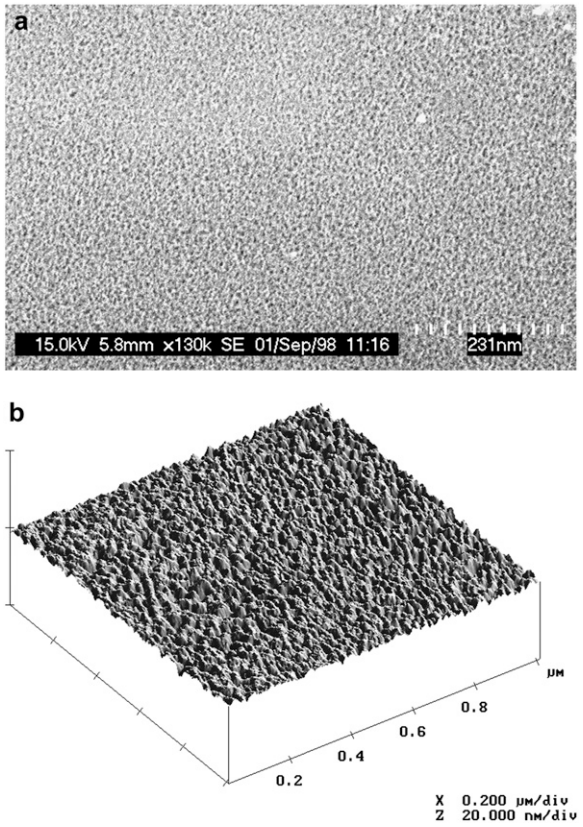

FIGURE 3 Images of the external surface of PS taken by SEM (*a*) and AFM (*b*).

The morphology of the surface is defined by the definite scaling rule: if $L' = kL$ then $w(L') = k^{\alpha}w(L)$ if L' and $L < L_{cl}$. The solution of this functional equation is well known:

$$w(L) = l\left(\frac{L}{l}\right)^{\alpha} f\left(\frac{L}{L_{cl}}\right), \quad f(x) = Const \quad \text{for} \quad x \ll 1,$$
$$f(x) = x^{-\alpha} \quad \text{for} \quad x \gg 1. \tag{1}$$

Here, the roughness exponent α is limited by the condition $0 < \alpha < 1$.

The longitude correlation length L_{cl} appears as a result of definite correlations during electrochemical etching of monocrystalline Si wafer and depends on etching conditions. L_{cl} is roughly 100 nm and can be expanded by an increase in etching time (9,10). The surface width $w(L)$ may be regarded as a measure of the correlation scale in the direction perpendicular to the referent surface (14). According to the definition of the self-affine surface, this scale depends on the size of the averaging section. Its maximal value is the correlation length L_{cp} in the direction perpendicular to the referent plane: $w(L \to \infty) \equiv L_{cp}$. Thus, according to Eq. 1,

$$L_{cp} = L_{cl}(L_{cl}/l)^{\alpha-1}, \tag{2}$$

and $L_{cp} \ll L_{cl}$ because the roughness exponent $0 < \alpha < 1$ and the minimal scale of self-similarity $l \ll L_{cl}$. For PS, L_{cp} is of the order of the mean pore size $\langle L_{c,pore} \rangle$ because the surface roughness is due to the pores etched on a fragment $L \times L$.

Using the above definitions, we will show that due to the fractal properties, local high supersaturation conditions can be created near the PS surface in the metastable solution. Supersaturation is a necessary, but not sufficient, condition for spontaneous nucleation: a free energy barrier of entropic origin must be overcome for a critical nucleus to form. An obvious way to promote nucleation is by inducing a local supersaturation spike, thus lowering the barrier at ideally one place in the medium, which will be the point where the critical nucleus forms. Naturally, the spatial size of this local spike should not be less than the size of the critical nucleus. A substrate that would locally increase the concentration of the molecules to be crystallized, with respect to the bulk, may therefore be an effective promoter of heterogeneous nucleation. The substrate does not need to be a postcritical nucleus (i.e., a seed crystal) itself, nor to be able to simultaneously constrain the minimal number of molecules that are necessary for criticality. A limited constraint, leading to a small increase in the probability of critical nucleus formation at the substrate, may be sufficient to induce crystallization if the system is not too far from labile conditions.

A high local supersaturation is possible near any surface if attractive forces are large enough. These conditions are realized in the cases of capillary condensation of neutral particles (15,16) and adsorption of charged particles on an oppositely charged surface (17). The attractive force between opposite charges of a molecule and a surface can produce a sufficiently large difference in surface free energy to produce sufficient local supersaturation of the charged particles, resulting in heterogeneous nucleation (17). Charged surfaces, including functionalized self-assembled monolayers (18), doped silicon microfluidic devices (19), poly-L-lysin covered glass surfaces (20), and charged beads like Sephadex and various zeolites, which combine charge with an ordinary regular porous structure (21), have all been tested as nucleation promoters. Most of these have been particularly successful with lysozyme, an easily crystallizable, fairly compact protein with a high surface charge density when at crystallization conditions. Success with a wider range of proteins has not been forthcoming and therefore such surfaces and beads have not gained widespread use.

Hydrophobic surfaces have also been shown to promote nucleation in some cases, possibly due to preferential binding of the few hydrophobic residues on the protein surface with the nucleant surface (22). This, however, is not true in general: hydrophobic surfaces are commonly used as inert substrates for protein crystallization by homogeneous nucleation.

A nucleation promoter can also be one that provides a template for epitaxial crystal growth. This is the obvious mechanism of one of the most common methods of improving macromolecular crystals, namely, seeding metastable solutions with a previously obtained small crystal of the sample (homologous seeding). Heteroepitaxial growth on minerals has also been attempted for protein crystallization (23). The presence of a heteroepitaxial growth mechanism has been demonstrated, but no single mineral has been found that can be used for a variety of different proteins. Hence, this arduous route has been largely abandoned by the macromolecular crystallographic community, for the moment at least.

In sum, it has been argued that a series of interactions may drive sufficient local supersaturation to lead to heterogeneous nucleation. These range from attraction between net opposite charges to short-range specific and nonspecific interactions (24), dispersion forces (17), hydrophobicity, etc.

For the most obvious case of attraction between net opposite charges, the signs of net molecular charge and surface charge are crucial for crystallization (17,19). However, the results of Chayen et al. (2) are independent of charge sign since the proteins under investigation had different net charge signs, yet crystallized on the same PS samples. The precise origin of the attraction potential is thus likely to vary between proteins, and it is not the purpose of this work to discuss it further.

We consider here the case where there is a definite attraction potential between proteins and silicon surface resulting in protein accumulation on the surface layer at a concentration higher than in the solution bulk (positive adsorption (25)) but still not sufficient for heterogeneous nucleation on a flat surface. We have focused on the fractal properties of PS surfaces, which—provided that some kind of sufficiently attractive potential is present—make it a more effective and wide-ranging nucleant than (functionalized) flat surfaces or surfaces with an ordinary regular porous structure.

RESULTS AND DISCUSSION

The mechanism suggested here is based on the specifics of any self-similar and self-affine fractal surfaces. For our purpose, it is convenient to characterize the fractal surface by the box-counting method (13). In the framework of this method, the fractality of the surface means that the number of particles $N_R(L)$ of size R required for monolayer coverage of a square fragment with edge length L increases with L faster than $(L/R)^2$:

$$N_R(L) = \left(\frac{L}{R}\right)^D f\left(\frac{L}{L_c}\right) \text{ with } f(x) = \text{Const for } x \ll 1 \text{ and}$$
$$f(x) = x^{-(D-2)} \text{ for } x \gg 1. \quad (3)$$

L here refers to the shortest distance between two adjacent corners of the fragment, not to the length of the cross sectional fractal curve; $D > 2$ is the fractal dimension of the

surface. In the case of self-affine surface, $D = 3 - \alpha$. The correlation length $L_c = L_{c,pore}$ and $l < R < min(L, L_{c,pore})$ for a self-similar pore surface. In the case of a self-affine surface, $L_c = L_{cl}$ and $l < R < w(L) < min(L, L_{cp}, L_{cl})$.

Equation 3 accounts for the well-known effect that $N_R(L)/L^2$ for particles deposited on fractal surfaces with the same fractal dimension D has different values due to different upper limits L_c of the fractal regime (26)—the greater the correlation scale L_c, the higher that quantity:

$$\frac{N_R(L)}{L^2} = \frac{1}{R^2}\left(\frac{L}{R}\right)^{D-2} f\left(\frac{L}{L_c}\right). \quad (4)$$

Note that the quantity $N_R(L)/L^2$ is an intensive thermodynamic variable (i.e., one independent of the size of averaging region L) for representative volume only ($L \gg L_c$). We call this quantity projected effective density, n_{ef}. It corresponds to the density of the projection onto a flat surface (of area $L \times L$) of a set of particles lying on the corrugated surface. As is clear from Eq. 4, n_{ef} is much higher than that on a regular surface: since $D > 2$ and $L_c \gg R$, it results that $n_{ef} \gg 1/R^2$, where R^{-2} would be the surface density on a flat surface for a complete monolayer.

We are exploiting this effect for the case of molecular ion adsorption from solution. We certainly do not have a complete monolayer due to mutual repulsion of the ions, and the mean distance between adsorbed ions can be greater than their size. Nevertheless, an effect analogous to that described by Eq. 3 is possible. Let the density of adsorbed molecules on a flat surface be n_s and the mean distance $n_s^{-1/2}$ between absorbed particles be less than L_c: ($n_s^{-1/2} \ll L_c$). The value of n_s depends on the concentration of particles in the metastable solution, interaction between the particles, and interaction of the particles with the surface. Certainly, we suppose that positive adsorption takes place (25), i.e., the mean distance $n_s^{-1/2}$ between absorbed particles is less than the mean distance between solute particles in the solution volume. So, $n_s^{-1/2}$ is a natural spatial scale for our model, and all distances will be measured in these units.

We can then speak of monolayer covering of the surface by ''particles'' of size $n_s^{-1/2}$. Thus, the effective projected density n_{ef} of these particles lying on the fractal surface is much higher than their density n_s on a regular surface:

$$n_{ef} = n_s\left(n_s L_c^2\right)^{(D-2)/2} \gg n_s, \quad (5)$$

when $n_s L_c^2 \gg 1$. The effect is absent if the molecule concentration in solution is not high enough and the mean distance $n_s^{-1/2}$ between absorbed particles on the flat surface is much more than L_c ($n_s^{-1/2} \gg L_c$). Since the correlation scale L_c is defined by the PS preparation conditions, it is possible to select the value of L_c for any concentration of metastable solution for the local density n_{ef} to be above metastability.

From simple geometric considerations, a higher n_{ef} implies a shorter average interparticle distance in physical (3D) space for the same average interparticle distance along the surface (i.e., on a two-dimensional metric attached to the surface). This can be intuitively pictured as follows: imagine a corrugated surface with particles rigidly fixed to it at given distances. This surface is now stretched out until completely flat, but no more. If the particles have remained fixed with respect to the surface, they will find themselves at greater distances from each other in 3D space than when the surface was corrugated. So, even if the actual surface density of the molecules on the fractal surface remains the same as on a flat surface, a higher n_{ef} means that the molecules are still brought much closer together than they would be if they were lying on the flat surface. Thus, in the vicinity of the fractal surface fragment, the effective surface density of protein molecules will be greater than in the vicinity of the flat surface.

Since we are interested in heterogeneous nucleation, let us show that the real local volume concentration $n_{v,loc}$ in the vicinity of the fractal surface is greater than in the vicinity of a flat surface. Moreover, this concentration should be no less than a critical concentration for spontaneous nucleation at given pressure P and temperature T, $n_{cr}(P, T)$. Naturally, the thickness z of this near-surface layer is no less than the size of the critical nucleus r_{cr}, $z \geq r_{cr}$ at the same time or $z \leq L_{cp}$ because we would like to use scaling relation Eq. 3. Here L_{cp} is the correlation length in the direction perpendicular to the referent plane of the self-affine surface if we are considering supersaturation in the vicinity of this surface and $L_{cp} = L_{c,pore}$ if we are considering supersaturation inside the pore.

So, the relation of scales for the layer is

$$l < R < n_s^{-1/2} < z \leq L_{cp}. \quad (6)$$

Let us estimate the volume of this boundary layer $V_b(z)$ and the number $N(z)$ of particles that can be placed inside this layer.

According to the fractal surface definition (13) and Eq. 3 we can calculate $V_b(z)$ as a complete volume of $(L/z)^D$ boxes, each of volume equal to z^3:

$$V_b(z) = z^3(L/z)^D \sim z^{3-D}. \quad (7)$$

We would now like to arrange the particles inside this volume. Since z is the distance in physical (3D) space, there will be $z/n_s^{-1/2}$ layers of particles. The number of particles in each layer is defined by the surface fractality and is equal to $(L/n_s^{-1/2})^D$. So, the total number of particles is

$$N(z) = (z/n_s^{-1/2})(L/n_s^{-1/2})^D \sim z^1 (n_s^{-1/2})^{-(1+D)}. \quad (8)$$

The local volume density will therefore be

$$n_{v,loc}(z) = N(z)/V_b(z) = n_s^{3/2}(z/n_s^{-1/2})^{D-2} > n_s^{3/2} = n_{v,fl}(\text{since } z > n_s^{-1/2} \quad \text{and} \quad D > 2). \quad (9)$$

Here we suppose that the distance between particles in the direction normal to the flat surface coincides with distance $n_s^{-1/2}$ along the surface, i.e., the volume density near the flat

surface $n_{v,fl} = n_s^{3/2}$. In a more realistic case, the distance between particles in the direction normal to the surface may be more than $n_s^{-1/2}$ since adsorption force (for example, van der Waals dispersion force) decreases with z. However, this is not important for our estimates since we use the same conditions for the flat surface, too.

So, although the boundary layer volume increases as z^{3-D} ($3 - D < 1$ since $D > 2$), the number of particles inside the layer increases as z^1 (Eqs. 7 and 8). This is the reason for the increase of local volume density. Recall that this is the effect of being in the vicinity of a fractal surface, since it is necessary that the condition in Eq. 6 be fulfilled. These conditions are rather rigid since in reality, fractal behavior is typically based on a scaling range that spans 0.5–2 decades (27).

Strictly speaking, L^D should be replaced by the Hausdorff D-measure $m^D(\Sigma)$ for the fractal surface (13). Then the boundary layer volume $V_b(z)$ is expressed as

$$V_b(z) = B\, z^{3-D}. \tag{10}$$

Here prefactor B is proportional to the Hausdorff D-measure $m^D(\Sigma)$ for a fractal (self-affine or self-similar) surface Σ (28):

$$B = \pi^{(3-D)/2}[(4-D)\Gamma((5-D)/2)]^{-1}\, m^D(\Sigma),$$
$$\pi^{(3-D)/2}[(4-D)\Gamma((5-D)/2)]^{-1} \approx 1. \tag{11}$$

The number of particles $N(z)$ inside the volume $V_b(z)$ is equal to the product of the number of layers with thickness $n_s^{-1/2}$ and the number of particles inside one layer, $N_s = m^D(\Sigma) n_s^{D/2}$:

$$N(z) = (z/n_s^{-1/2})\, m^D(\Sigma)\, n_s^{D/2}. \tag{12}$$

So, the local particle density $n_v(z) = N(z)/V_b(z)$ inside a boundary layer of thickness z near fractal surface with fractal dimension D depends on D and z only and is independent of the Hausdorff D-measure

$$n_{v,loc}(z) = \frac{1}{n_s^{-3/2}}\left(\frac{z}{n_s^{-1/2}}\right)^{D-2} = n_{v,fl}(n_s z^2)^{(D-2)/2} > n_{v,fl}. \tag{13}$$

We can see that the results of Eqs. 9 and 13 are identical. It is more convenient to operate with a fragment of the surface with lateral size L. It is known that the Hausdorff D-measure $m^D(\Sigma) \le L^D$. Since the effective density $n_V(z)$ is independent of $m^D(\Sigma)$ we prefer the simplest form for $N(z)$ and $V_b(z)$: $N(z) = (z/n_s^{-1/2}) L^D n_s^{-D/2}, V_b(z) = z^3 (L/z)^D$.

Thus, any fractal substrate yields a sufficient local concentration for nucleation if the following conditions are fulfilled:

$$n_{v,loc}(L_{cp}) = n_{v,fl}(n_s^{1/2} L_{cp})^{(D-2)} > n_{cr}(P,T) \quad \text{and}$$
$$R < n_s^{-1/2} < L_{cp}, D > 2. \tag{14}$$

Here $n_{cr}(P, T)$ is a critical concentration for spontaneous nucleation at given pressure P and temperature T. The conditions in Eq. 14 let us make an optimal choice of crystallization and substrate-related parameters for heterogeneous nucleation of any protein. Indeed, n_s is a function of solution metastability and silicon-protein interaction, whereas fractal dimension D and correlation length L_c are controlled by fabrication conditions. It was shown that the fractal dimension D, reflecting surface morphology of individual pore and the whole structure of porous network, is strongly porosity dependent (12). For example, its value can be changed from 2.1 to 2.4 for porosity range 40–70%, indicating an increase of nanocrystallite roughness and, consequently, the specific surface area with porosity (12). In turn, the correlation length L_c was shown to be a function of anodization time (9,10). The pore size which serves as a correlation length for an individual fractal pore can be varied from nanometer to micrometer scale. Practically, the pore size as well as the porosity can be changed by varying the anodization current density, HF solution concentration as well as doping type and level of the starting silicon substrate (29,30). So, we can select favorable fabrication parameters to tailor fractal dimension D and correlation length L_c for a given protein to satisfy nucleation conditions. Assuming that useful pores for our purposes range in size from the diameter of a protein molecule to that of a critical nucleus, we would like to have a pore size distribution that ranges over a few protein diameters.

It remains however to be judged whether a very wide, ''nontailored'' and therefore more ''universal'' pore size distribution is to be preferred over a more protein-adapted 'tailored' surface. A broad distribution of fractal pore sizes in PS sample may indeed be a crucial advantage, in providing for each of various proteins the pore size most suited to its molecular diameter and to the shape of the initial aggregates that it forms. On the same PS surface, different pores provide different supersaturation conditions for a given protein molecule because of the variation of the fractal parameters. Hence, the same PS can serve as a nucleant for various protein molecules. To reach conclusions on this matter, more crystallization experience with this and possibly other similar materials will doubtless be required.

CONCLUSIONS

PS appears to be an effective nucleant for protein crystallization, due to its fractal properties. The fractal structure of PS provides the local supersaturation spike needed for the heterogeneous nucleation of molecules from metastable solutions.

Local supersaturation ''spikes'' are not in themselves sufficient to guarantee successful crystal growth, especially where macromolecular crystals are concerned. For crystal nucleation, rather than the triggering of phase separation or precipitation/amorphous aggregation, the protein solution has to be metastable with respect to a crystalline phase. In other words, the protein solution must be close to conditions

where the protein would crystallize spontaneously in the absence of a nucleant. Practically, this means that the specific interactions between protein molecules (the ones that lead to 3D crystal formation) must be of comparable magnitude to the protein-nucleant attraction. If protein-protein interactions are too weak at the given conditions, then deposition of molecules on the nucleant surface will at best be achieved. If the interactions are not specific and conducive to ordered packing, then only amorphous aggregation can result.

These caveats should not detract from the importance of heterogeneous nucleation, which has two advantages. First, nucleation and growth at metastable conditions is highly advantageous because the effects of spontaneous nucleation are prevented. The slower growth and the lack of excess and secondary nucleation often provide for growth of larger, better diffracting crystals (17). Second, the probability of a 'hit' in the usual trial-and-error initial crystallization screening of a protein is increased, since metastable conditions will also yield crystals in the presence of the heterogeneous nucleant whereas they would remain clear in the absence of nucleant.

Our model shows that a sufficient local concentration of molecules for nucleation is possible inside and in the close vicinity of the pores, even when the average conditions in the bulk of the solution correspond to metastability. Whatever the mechanism of molecule adsorption, with correct choice of crystallization and of surface-related parameters, heterogeneous nucleation may occur due to the local supersaturation at the fractal surface. The PS substrate can serve as a rather universal nucleant for various protein molecules due to the wide distribution of fractal pore sizes. In addition, the PS technology is very flexible, allowing tailoring the pore size and concentration as well as the fractal properties to specific proteins by changing the fabrication conditions. It should be noted that heterogeneous nucleation of protein crystals never succeeded on oxidized PS, which had lost its fractal properties (11). This fact is probably an additional demonstration of the role of fractality in the promotion of heterogeneous nucleation.

According to our theory, this nucleation-promoting property of PS is more general and is not limited to amphoteric macromolecules only. Indeed, it was also observed in the case of enhanced crystallization and bonding of ceramics and oxides to PS surfaces (4,5). On the other hand, our consideration of the phenomenon of local supersaturation caused by fractality does not rely upon specific parameters of PS and may be applied to any fractal surface.

We gratefully acknowledge the support of the Kamea Program of the Ministry of Absorption, State of Israel.

REFERENCES

1. Chayen, N. E. 2004. Turning protein crystallization from an art into a science. *Curr. Opin. Struct. Biol.* 14:577–583.
2. Chayen, N. E., E. Saridakis, A. El-Bahar, and Y. Nemirovsky. 2001. Porous silicon: a nucleation inducing material for protein crystallization. *J. Mol. Biol.* 312:591–596.
3. Canham, L. T. 1997. Biomedical applications of porous silicon. *In* Properties of Porous Silicon. L. Canham, editor. EMIS Datareviews series No. 18, INSPEC. Institution of Engineering and Technology, London, UK. 371–376.
4. Stolyarova, S., A. El-Bahar, and Y. Nemirovsky. 2002. Unexpected room temperature growth of silicon dioxide crystallites on passivated porous silicon. *J. Cryst. Growth.* 237–239:1920–1925.
5. Stolyarova, S., B. Malic, S. Javoric, A. El-Bahar, M. Kosec, and Y. Nemirovsky. 2003. Integration of porous silicon with sol-gel derived ceramic films. *Proc. Mater. Res. Soc. Sym. USA.* 768:57–62.
6. Di Francia, G., V. La Ferrara, P. Maddalena, D. Ninno, L. P. Odierna, and V. Cataudella. 1996. AC conductivity of porous silicon: a fractal and surface transport mechanism. *Nuovo-Cimento.* D18:1187–1196.
7. Matthai, C. C., J. L. Gavartin, and A. A. Cafolla. 1995. Structural and elastic properties of porous silicon. *Thin Solid Films.* 255:174–176.
8. Aleksandrow, L. N., and P. L. Novikov. 1998. Mechanisms of formation and topological analysis of porous silicon - computational modeling. *Comput. Mater. Sci.* 10:406–410.
9. Happo, N., M. Imamatsu, and K. Horii. 2000. Self-affine fractal of porous silicon surface before and after natural oxidation. *Phys. Status Solidi A.* 182:233–237.
10. Happo, N., M. Fujiwara, M. Iwamatsu, and K. Horii. 1998. Atomic force microscopy study of self-affine fractal roughness of porous silicon surfaces. Jpn. J. Appl. Phys. 37:3951–3953.
11. Young, T. F., I. W. Huang, Y. L. Yang, W. C. Kuo, I. M. Jing, T. C. Chang, and C. Y. Chang. 1996. Atomic force microscopy study of the surface structure of oxidized porous silicon. *Appl. Surf. Sci.* 102: 404–407.
12. Nychyporuk, T., V. Lysenko, and D. Barbier. 2005. Fractal structure of porous silicon nanocrystallites. *Phys. Rev.* B71:1154021–1154025.
13. Gouyet, J.-F. 1996. Physics and Fractal Structures. Springer-Verlag, Berlin/Heidelberg, Germany.
14. Family, F. 1990. Dynamic scaling and phase transitions in interface growth. *Physica A.* 168:561–580.
15. Donley, J. P., and A. J. Liu. 1997. Phase behavior of near-critical fluids confined in periodic gels. *Phys. Rev. E.* 55:539–543.
16. Kunzner, N., E. Gross, J. Diener, D. Kovalev, V. Y. Timoshenko, and D. Wallacher. 2003. Capillary condensation monitored in birefringent porous silicon layers. *J. Appl. Phys.* 94:4913–4917.
17. Sear, R. P. 2003. Protein crystals and charged surfaces: interactions and heterogeneous nucleation. *Phys. Rev E.* 67:0619071–0619107.
18. Zhu, P., Y. Masuda, and K. Koumoto. 2004. The effect of surface charge on hydroxyapatite nucleation. *Biomaterials.* 25:3915–3921.
19. Sanjoh, A., and T. Tsukihara. 1999. Spatiotemporal protein crystal growth studies using microfluidic silicon devices. *J. Cryst. Growth.* 196:691–702.
20. Nanev, C. N., and D. Tsekova. 2000. Heterogeneous nucleation of hen-egg-white lysozyme—molecular approach. *Cryst. Res. Technol.* 35: 189–195.
21. Chayen, N. E., and E. Saridakis. 2001. Is lysozyme really the ideal model protein? *J. Cryst. Growth.* 232:262–264.
22. Tsekova, D., S. Dimitrova, and C. N. Nanev. 1999. Heterogeneous nucleation (and adhesion) of lysozyme crystals. *J. Cryst. Growth.* 196:229–233.
23. McPherson, A., and P. Shlichta. 1988. Heterogeneous and epitaxial nucleation of protein crystals on mineral surfaces. *Science.* 239: 385–387.
24. Falini, G., S. Fermani, G. Conforti, and A. Ripamonti. 2002. Protein crystallization on chemically modified mica surfaces. *Acta Crystallogr.* D58:1649–1652.
25. Landau, L. D., and E. M. Lifshitz. 1993. Statistical Physics. Pergamon Press, Oxford/New York/Seoul/Tokyo.

26. Pfeifer, P., Y. J. Wu, M. W. Cole, and J. Krim. 1989. Multilayer adsorption on a fractally rough surface. *Phys. Rev. Lett.* 62:1997–2000.

27. Malcai, O., D. A. Lidar, O. Biham, and D. Avnir. 1997. Scaling range and cutoffs in empirical fractals. *Phys. Rev. E.* 56:2817–2827.

28. Wong, Pz., and A. J. Bray. 1988. Porod scattering from fractal surfaces. *Phys. Rev. Lett.* 60:1344.

29. Halimaoui, J. 1997. Porous silicon formation by anodisation. *In* Properties of Porous Silicon. L. Canham, editor. EMIS Datareviews series No. 18, INSPEC. Institution of Engineering and Technology, London, UK. 12–22.

30. Herino, R. 1997. Pore size distribution in porous silicon. *In* Properties of Porous Silicon. L. Canham, editor. EMIS Datareviews series No. 18, INSPEC. Institution of Engineering and Technology, London, UK. 89–96.